JOURNAL OF Materials CHEMISTRY

Barium vanadium pentoxide-based compounds prepared *via* a sol–gel process and their evaluation as lithium intercalation materials

V. Vivier,[a] R. Baddour-Hadjean,[a†] J. P. Pereira-Ramos*[a] and N. Baffier[b]

[a]*Laboratoire d'Electrochimie, Catalyse et Synthèse Organique, CNRS UMR 28, 2 rue Henri Dunant 94320 Thiais, France*

[b]*Laboratoire de Chimie Appliquée de l'Etat Solide, CNRS URA 1466, 11 rue Pierre et Marie Curie, 75231 Paris Cedex, France*

The sol–gel process has allowed us to synthesize two new specimens of barium vanadium pentoxide-based compounds: (i) an oxidized orthorhombic Ba–V oxide (referred to as oxidized 'BVO'), whose formula $Ba_{0.18}V_2O_{5.15}$ is close to that of a mixed oxide; (ii) a reduced monoclinic Ba–V oxide (referred to as reduced 'BVO'), with formula $Ba_{0.18}V_2O_{4.95}$. Both materials are obtained after specific heat-treatment of the barium exchanged xerogel. The electrochemical features of lithium insertion in both compounds are reported. The oxidized and reduced 'BVO' have different and peculiar electrochemical behaviour, which is discussed in connection with that of the parent orthorhombic V_2O_5 oxide and the monoclinic $Na_{0.33}V_2O_5$ bronze, respectively.

Previous studies have outlined the interest in using the sol–gel process to prepare high performance cathodic materials for secondary lithium batteries.[1–3] Indeed, sol–gel chemistry offers a new approach to the synthesis of MnO_2-[4,5] and V_2O_5-[1,6–8] based compounds. Starting from molecular precursors, an oxide network is obtained *via* inorganic polymerization reactions in solution. The V_2O_5 group constitutes a wide variety of materials: gels, xerogels, oxides and bronzes. Their synthesis is described in ref. 1–3 and 6–8. Oxides and bronzes are obtained from the V_2O_5 xerogel (VXG). The latter is made of negatively charged ribbons and contains inter-ribbon protonated water; in this way, owing to its cationic exchange properties in aqueous solution, various ion exchanged xerogels can then be obtained. Further appropriate heat-treatment in air leads to bronzes or mixed oxides, depending on the nature of the cationic species and their degree of insertion. In the case of bronzes, a large amount of vanadium ions are reduced (*ca.* 0.33 V^{4+} mol^{-1} from heat-treatment in air). When monovalent cations such as sodium, potassium or silver ions have been previously exchanged in VXG, the corresponding monoclinic $M_xV_2O_5$ vanadium bronzes are obtained such as β-$Na_{0.33}V_2O_5$,[7] β-$K_{0.25}V_2O_5$[9] and β-$Ag_{0.3}V_2O_5$[3] while the formation of orthorhombic $M_xV_2O_{5+\varepsilon}$ mixed oxides is observed for trivalent iron(III)[10] or aluminium[11] ions.

In a previous study, the enhanced electrochemical behaviour (in terms of specific capacity and cycling efficiency) of the sodium bronze has been demonstrated and explained by the specific morphology induced by the sol–gel process.[7]

More recently, some of us have reported the electrochemical properties of the aluminium–vanadium mixed oxide[11] as well as the promising behaviour of a new iron–vanadium mixed oxide as rechargeable positive electrode for Li batteries.[10,12] For instance, a notable improvement in cycle life was found compared with the parent oxide V_2O_5.

These results prompted us to investigate the influence of a divalent and large size cation such as Ba^{2+} on the structural and electrochemical properties of the corresponding sol–gel barium V_2O_5-based compounds.

Barium vanadium bronzes have been reported for the first time by Fotiev *et al.*[13,14] Three compounds, classified among the oxygen vanadium bronzes, have been synthesized using solid-state reactions at high temperature. They are referred to as $BaV_{12}O_{30}$ (α phase), BaV_8O_{21-x} (β phase) and $Ba_3V_4O_{13}$ (δ phase). However, the structure of these various materials is not clearly defined. Very recently, a new monoclinic barium vanadium bronze derived from the parent V_3O_8 oxide has been hydrothermally synthesized.[15] Nevertheless, none of these Ba–V oxides have been evaluated as Li intercalation materials so far. Here we report the structural and electrochemical features of two new barium V_2O_5-based compounds synthesized *via* the sol–gel process.

Experimental

Preparative procedure

The basic material, the V_2O_5 gel, with formula $V_2O_5{\cdot}nH_2O$, is prepared by spontaneous polycondensation of decavanadic acid.[8] The sol–gel process is based on the acidification of a metavanadate solution by passing it through an ion exchange resin. Gelation is observed when the vanadium concentration is higher than 0.1 M. Deposited on glass plates, the red viscous gel loses most of its water molecules at room temperature, leading to thin films of V_2O_5 xerogel (VXG), with the following schematic formula:[6]

$$(V_2O_{5.16})^{0.33-}{\cdot}0.33H_3O^+{\cdot}xH_2O\ (x \approx 1.3)$$

VXG is made of negatively charged ribbons between which are located hydronium ions [*ca.* 0.33 (mol oxide)$^{-1}$]. The latter ensure the global electroneutrality and constitute the ionic exchange capacity of the xerogel. The water content (*ca.* 1.3 mol^{-1}) splits into inter-ribbon water (*ca.* 1.1 mol^{-1}) and strongly bonded structural water (*ca.* 0.2 mol^{-1}).

A quantitative ion exchange procedure performed in a 0.1 M $BaCl_2$ or $Ba(NO_3)_2$ aqueous solution allows the corresponding barium xerogel[16,17] to be obtained. Then, two distinct heat treatments were performed on the exchanged xerogel: one at 520 °C in air, the other at 520 °C in a hydrogenated atmosphere (Ar–10% H_2). Both give rise to the formation of solid products, consisting of platelets of a few micrometers thick (Fig. 1).

The barium contents in the two final materials were determined by atomic absorption experiments. The same value is obtained for both compounds: 0.18 Ba (mol V_2O_5)$^{-1}$. This corresponds to 0.36 positive charges (mol oxide)$^{-1}$, which is consistent with the VXG ionic exchange capacity.

The amount of V^{4+} in each sample was evaluated by redox

† Present adress: LASIR, CNRS, UPR 2631, 2 rue Henri Dunant 94320 Thiais, France.

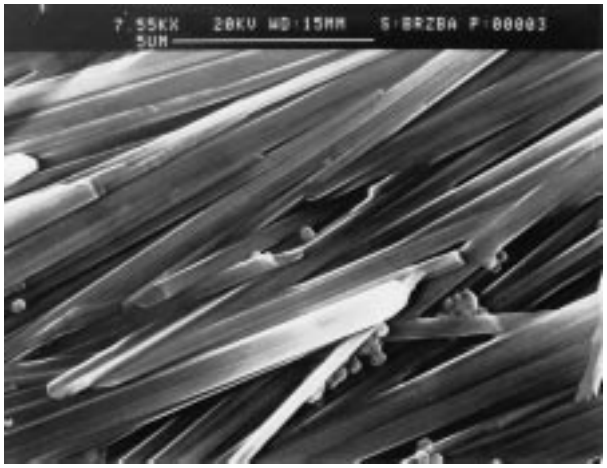

Fig. 1 SEM micrograph (×7500) of the barium vanadium oxide $Ba_{0.18}V_2O_{5.15}$

chemical analysis. Heat treatment in air leads to the oxidized 'BVO' with formula: $Ba^{2+}{}_{0.18}V^{5+}{}_{1.94}V^{4+}{}_{0.06}O^{2-}{}_{5.15}$, and low initial V^{4+} content (*ca.* 3%), whereas heat treatment in a hydrogenated atmosphere leads to a reduced 'BVO' with formula $Ba^{2+}{}_{0.18}V^{5+}{}_{1.54}V^{4+}{}_{0.46}O^{2-}{}_{4.95}$. The larger amount of V^{4+} found in the reduced 'BVO' (*ca.* 23%) is induced by the hydrogenated atmosphere during heat treatment. This leads to a mean oxidation degree of 4.77 for the vanadium ion in the reduced 'BVO' compared to 4.83 in the sodium bronze obtained in an air atmosphere

The sol–gel barium compounds will be referred to as $Ba_{0.18}V_2O_{5.15}$ for the oxidized 'BVO' and $Ba_{0.18}V_2O_{4.95}$ for the reduced 'BVO'.

X-Ray diffraction experiments were performed with an INEL diffractometer using Cu-Kα_1 radiation.

Electrochemical measurements

Propylene carbonate (PC), twice distilled, was obtained from Fluka. Anhydrous lithium perchlorate was dried under vacuum at 200 °C for 12 h. The electrolytes were prepared under a purified argon atmosphere. Electrochemical measurements were performed in a conventional three-electrode cell with flooded electrolyte. The working electrode consisted of a stainless steel grid with a geometric area of 1 cm^2 on which *ca.* 20 mg of material mixed with graphite (90 mass%) was pressed. For kinetic measurements, the cathodic material was made of platelets of pure material sandwiched between two gold grids. Lithium was used as the reference and auxiliary electrodes. Impedance spectroscopy was carried out in the frequency range 10^{-3}–10^4 Hz using an EGG (PAR) Model 273A electrochemical system coupled with a 1255 Schlumberger Frequency Response Analyser. The excitation signal on the system at the equilibrium potential was 10 mV peak to peak. The equilibrium potential was considered to be reached when the drift in open-circuit voltage remained <1 mV over 2 h. Similar conditions have been applied to obtain the OCV curve $E=f(x)$.

Results and Discussion

Structure of the sol–gel barium compounds

The X-ray diffraction pattern in reflection geometry of the barium intercalated xerogel is shown in Fig. 2(*a*). As previously observed,[16,17] this compound exhibits a highly preferred 00*l* orientation corresponding to the stacking of the ribbons along the *c* direction. The corresponding interlamellar distance is 11.2 Å with one water layer. The Ba^{2+} ion is the only case of a divalent ion with a single water layer. This result has to be

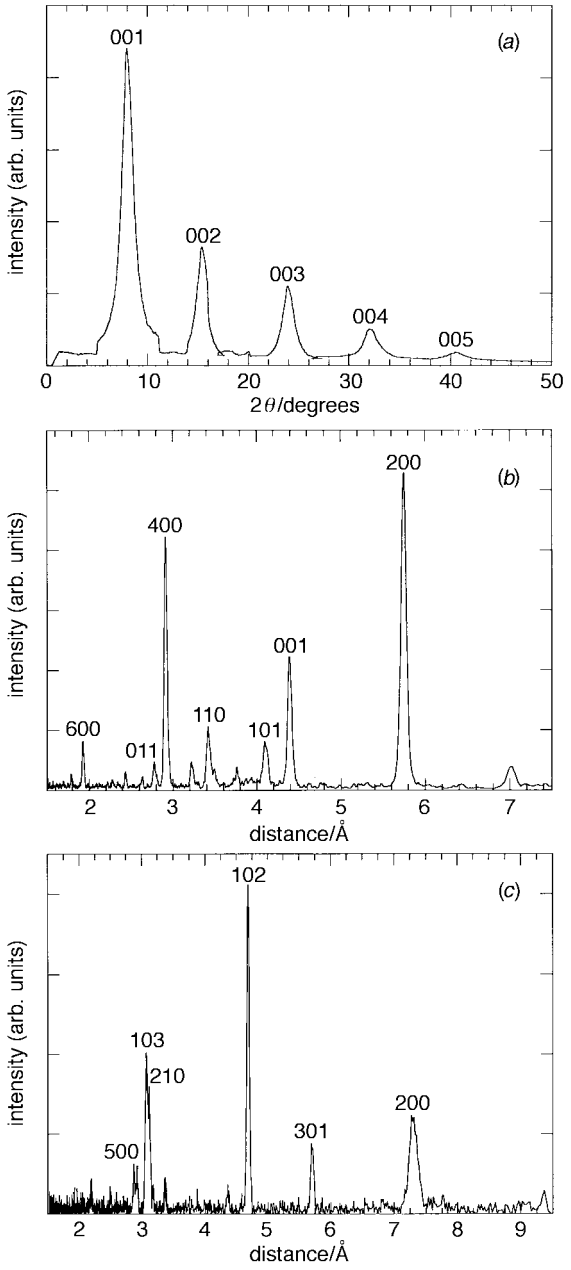

Fig. 2 X-Ray diffraction patterns in reflection geometry of: (*a*) the barium intercalated xerogel; (*b*) the previously ground sol–gel $Ba_{0.18}V_2O_{5.15}$; (*c*) the previously ground sol–gel $Ba_{0.18}V_2O_{4.95}$

correlated to the charge to radius ratio of the Ba^{2+} ion which tends to reduce the number of water molecules around it.[18]

The X-ray diffraction pattern in reflection geometry performed on the previously ground sol–gel $Ba_{0.18}V_2O_{5.15}$ [Fig. 2(*b*)] is typical of an orthorhombic structure.[16,17] The space group is *Pmmm* and the lattice parameters ($a=11.53$, $b=3.56$, $c=4.38$ Å) are very nearly the same as those of the parent orthorhombic V_2O_5 oxide.

It appears that even though the oxidized 'BVO' has been ground, the Bragg peaks 200 and 400 have significant intensities, which indicates a preferred orientation for the stacking of the (100) planes.

Finally, we obtain an orthorhombic phase $Ba_{0.18}V_2O_{5.15}$, quite different from Fotiev's results which described for the nearly same barium content a monoclinic α $BaV_{12}O_{30}$ phase isostructural with $Na_2V_{12}O_{30}$.[14]

The X-ray diffraction pattern of the previously ground sol–gel $Ba_{0.18}V_2O_{4.95}$ is shown in Fig. 2(*c*). The crystallographic parameters have been refined by indexation of the XRD powder spectrum (DicVol 91 refinement procedure):

Table 1 X-Ray diffraction parameters (angles and intensities) for BaV_8O_{21-x}[14] and $Ba_{0.18}V_2O_{4.95}$ (this work)

BaV_8O_{21-x}	$Ba_{0.18}V_2O_{4.95}$		
d/Å	intensity	d/Å	hkl
7.28	60	7.28	2 0 0
—		5.7	3 0 −1
4.74	100	4.74	1 0 −2
—		4.38	2 0 1
3.36	60	3.36	5 0 −2
3.2	20	3.2	2 1 −1
3.15	60	3.15	2 1 0
3.05	40	3.05	1 0 −3
2.91	80	2.91	5 0 0
2.7	20	2.7	4 1 −1
2.51	20	2.51	1 0 3
2.37	20	2.37	2 0 −4
2.16	60	2.16	6 1 −1
1.96	40	1.96	4 0 −5
1.8	60	1.8	0 1 4
1.53	20	1.53	4 2 −3
1.48	40	1.48	5 1 −6
1.38	20	1.38	4 1 4

$Ba_{0.18}V_2O_{4.95}$ has a monoclinic structure, as observed for the monovalent bronzes $Na_{0.33}V_2O_5$[7] and $K_{0.25}V_2O_5$.[9] Nevertheless, the lattice parameters and possible space groups ($P2$, $P2/m$ or Pm) are quite different: $a=9.845$, $b=3.495$, $c=17.11$ Å, $\beta=121.73$ °C.

This deviation is not striking when considering the following: (i) the 'anomalous' high V^{4+} content in the reduced 'BVO' (0.46 V^{4+} mol^{-1}) compared to the lower value usually found for monoclinic bronzes obtained from heat-treatment in air (0.33 V^{4+} mol^{-1}); (ii) the large size of the barium ion as intercalated species and (iii) the oxygen-deficient formula of the reduced 'BVO'.

As the angles and the intensities of the $Ba_{0.18}V_2O_{4.95}$ diffraction peaks turn out very similar to those previously found for the β phase BaV_8O_{21-x} ($Ba_{0.25}V_2O_{5.25-\varepsilon}$) (Table 1),[14] the sol–gel $Ba_{0.18}V_2O_{4.95}$ and the solid-state synthesized $Ba_{0.25}V_2O_{5.25-\varepsilon}$ might exhibit similar crystalline structure. However, neither X-ray indexation, nor crystalline parameters are reported for the solid-state β phase. An orthorhombic structure is proposed from optical measurements.[14]

The chemical formula given for the $Ba_{0.25}V_2O_{5.25-\varepsilon}$ bronze prepared *via* solid-state reactions must be questioned as it is not confirmed by the chemical analysis of the V^{4+} content (ε). This formula does not account for the presence of a reduced oxide, but rather for a mixed oxide in which additional 0.25 oxygen atoms are introduced to counterbalance the positive charge of the barium ions.

Electrochemical properties

(a) The oxidized 'BVO' $Ba_{0.18}V_2O_{5.15}$. The evolution of the equilibrium potential obtained at 20 °C for the first two steps of lithium insertion in $Ba_{0.18}V_2O_{5.15}$ is compared with the V_2O_5 parent oxide (Fig. 3). The first two well defined insertion processes at 3.3 and 3.2 V usually described for V_2O_5 are barely defined for the barium oxide, even if a similar shape is observed for both compounds.

Fig. 4 shows the chronopotentiometric reduction curve obtained at 150 °C for the oxidized 'BVO' compared to that of the V_2O_5 oxide. A single step is observed for the barium oxide in the potential range 3.5–3 V, owing to the high current density (1 mA cm^{-2}). However, two additional lithium insertion processes are found at 2.3 and 2.1 V for both compounds. This provides the electrochemical fingerprint of the orthorhombic symmetry of $Ba_{0.18}V_2O_{5.15}$, as reported previously for other vanadium oxides.[10–12] For a 3 V cut-off voltage, about 0.45 Li ions are accommodated in $Ba_{0.18}V_2O_{5.15}$ *cf. ca.* 0.95 in V_2O_5.

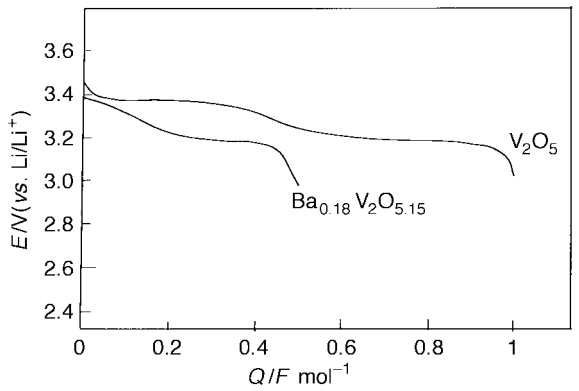

Fig. 3 OCV curves for the first two steps of lithium intercalation at 20 °C in $Ba_{0.18}V_2O_{5.15}$ and V_2O_5

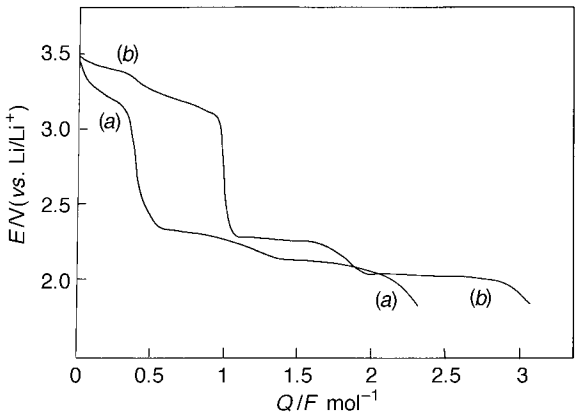

Fig. 4 Chronopotentiometric curves at 150 °C for the reduction at constant current density (1 mA cm^{-2}) of (*a*) $Ba_{0.18}V_2O_{5.15}$, (*b*) V_2O_5 in 1 mol kg^{-1} $LiClO_4$–DMSO

The lithium capacity is shown to be significantly temperature dependent (0.2–0.6 F mol^{-1} for a 3 V cut-off voltage between 20 and 150 °C), which suggests important kinetic limitations in the barium–vanadium oxide. Nevertheless, the maximum lithium uptake remains significantly lower than the theoretical value expected in the potential range 3.5–3 V. The reduced faradaic yield might stem from the presence of additional ions (oxygen and/or barium) located between the V_2O_5 slabs in the sites usually available for lithium intercalation. Such an atomic distribution would differ from that reported for the orthorhombic $Fe_{0.11}V_2O_{5.16}$ mixed oxide. In the latter compound, trivalent iron ions are found to be located in octahedral positions in the plane of the V_2O_5 sheets.[12] The presence of barium ions between the V_2O_5 slabs in $Ba_{0.18}V_2O_{5.15}$ is supported by the divalent charge and the size of the barium ion. This assumption needs to be checked by further structural investigations.

Finally, we have investigated the lithium chemical diffusion coefficient in the oxidized 'BVO', using the current-pulse relaxation technique described by Basu and Worrel,[19] and ac impedance. As previously reported,[11] the complementary use of both methods allows discrimination in frequencies (*e.g.* in time) of the different limiting processes, leading to reliable $\tilde{D}_{Li}$ values.

Experimental data found for the chemical diffusion coefficient of Li^+ ions as a function of x in $Li_xBa_{0.18}V_2O_{5.15}$ are presented in Table 2. Three sets of data, in the range 10^{-10}, 10^{-11} and 10^{-12} cm^2 s^{-1} are observed in the 0–0.1, 0.1–0.2 and 0.2–0.35 composition ranges respectively. Comparison with the $\tilde{D}_{Li}$ values reported for the closely related orthorhombic oxides V_2O_5[20] and $Al_{0.11}V_2O_{5.15}$,[11] in the range 10^{-9}–10^{-11} cm^2 s^{-1}, highlights the fact that, unlike these oxides, lithium diffusion in the barium oxide is rapidly diminished (from $x\approx0.2$), as a result of important repulsive

Table 2 Variation of the chemical diffusion coefficient of lithium $\tilde{D}_{Li}$ as a function of x in $Li_xBa_{0.18}V_2O_{5.15}$

x	$\tilde{D}_{Li}/cm^2\ s^{-1}$
0.05	1×10^{-10}
0.1	3×10^{-10}
0.15	1.5×10^{-11}
0.2	5×10^{-11}
0.25	1×10^{-12}
0.3	1×10^{-12}
0.35	1×10^{-12}

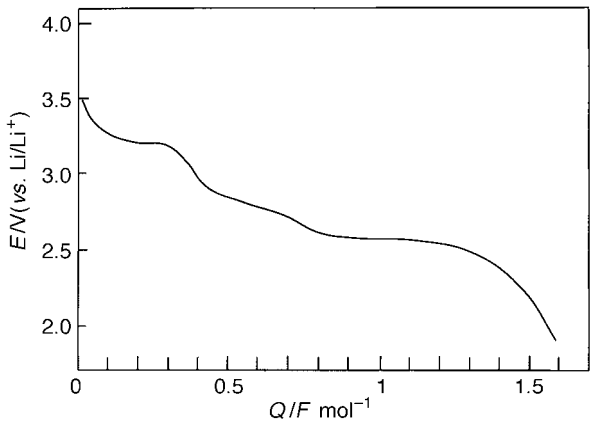

Fig. 5 Chronopotentiometric curve at 20 °C for the reduction at constant current density $C/10$ (50 μA cm^{-2}) of $Ba_{0.18}V_2O_{4.95}$ in 1 M $LiClO_4$–PC

coulombic interactions combined with the size of the inserted barium ions.

This is consistent with the strong influence of the temperature on the electrochemical behaviour described above.

(b) The reduced 'BVO' $Ba_{0.18}V_2O_{4.95}$. Electrochemical lithium insertion at moderate constant current density ($C/10$) in $Ba_{0.18}V_2O_{4.95}$ (Fig. 5) involves three main steps in the potential window 3.7–2 V separated by smooth potential drops for *ca.* $x=0.3$ and $x=0.7$ lithium ions per mole of oxide. At first, the working potential varies continuously from 3.5–3.25 V for $0<x<0.15$ and then with a lower slope up to $x=0.3$ (3.15 V). Thereafter, two steps are observed near 2.8 and 2.6 V, involving the insertion of 0.33 and 0.95 Li^+ ions, respectively, which leads to a total faradaic yield of 1.54 F mol^{-1}. This value confirms the initial presence of *ca.* 0.46 V^{4+} ions mol^{-1} in the reduced 'BVO', leading to only 1.54 reducible V^{5+} ions in this potential range.

The shape of the chronopotentiometric curve for the reduction of $Ba_{0.18}V_2O_{4.95}$ (Fig. 5) is closely related to the electrochemical features usually observed for other sol–gel or classically prepared monoclinic bronzes such as $Na_{0.33}V_2O_5$[7,21] and $K_{0.25}V_2O_5$.[9] It consists of three well defined reversible insertion steps at average potentials of 3.3, 2.9 and 2.55 V within the composition ranges $0<x\leqslant0.33$–0.4, 0.35–$0.4<x\leqslant0.7$–0.75 and 0.7–$0.75<x\leqslant1.65$–1.75, respectively.

We may therefore assume that there are three kinds of lithium insertion sites in the reduced 'BVO', as previously reported for the sodium compound.[22] Moreover, the shape of the electrochemical reduction curve indicates that the filling of these sites occurs at the same energy levels for the barium and the sodium compounds. Further informations on the filling scheme of lithium in $Ba_{0.18}V_2O_{4.95}$ requires determination of both the position and the symmetry of the insertion sites.

The influence of the current density in the range 0.05–0.5 mA cm^{-2} on the discharge curve of the reduced 'BVO' is shown in Fig. 6. The electrochemical properties are strongly

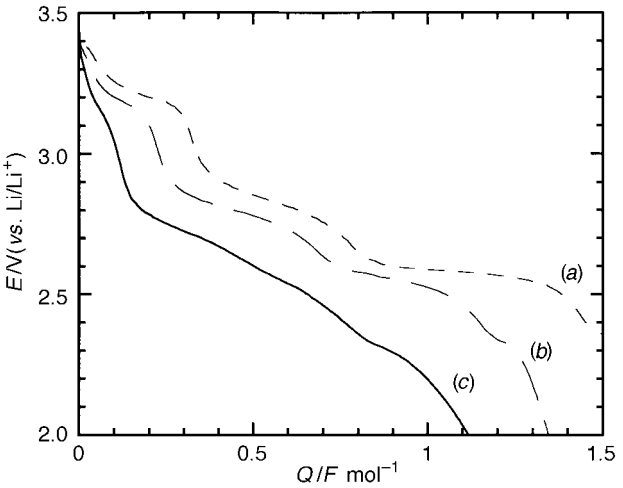

Fig. 6 Influence of the current density (in mA cm^{-2}) on the discharge curves of $Ba_{0.18}V_2O_{4.95}$ electrodes: (*a*) 0.05, (*b*) 0.1, (*c*) 0.5

affected since both the working potential and the faradaic yield decrease as the current density increases. These important kinetic limitations for lithium transport in the host structure of the reduced 'BVO' probably originate from stronger barium–lithium interactions than those encountered in the sodium bronze, particularly for the lowest lithium contents.

Finally, cyclic galvanostatic experiments have been performed in a potential range including either the first three lithium insertion steps (Fig. 7), or the first two lithium insertion steps (Fig. 8). As shown in Fig. 7, when cycling includes all three steps, the specific capacity recovered continuously decreases with the number of cycles (60% of its initial value after 5 cycles). However, restricting to the cycling limits in the potential range 4–2.7 V (including only the first two steps) leads to a notable improvement. After the first discharge, a specific capacity of *ca.* 0.5 F mol^{-1} remains stable over at least 50 cycles (see Fig. 8).

One should also note that whatever the cut-off voltage, the capacity recovered during reduction can never be totally recovered during oxidation. The loss (0.2–0.3 F mol^{-1}) would correspond to residual lithium ions irreversibly trapped in the host structure of the reduced 'BVO'.

The XRD spectrum of the partially deintercalated sample ($x=0.22$) previously charged up to $x=1.6$ does not reflect this as it shows the restoration of the initial structure, in spite of the poor electrochemical reversibility.

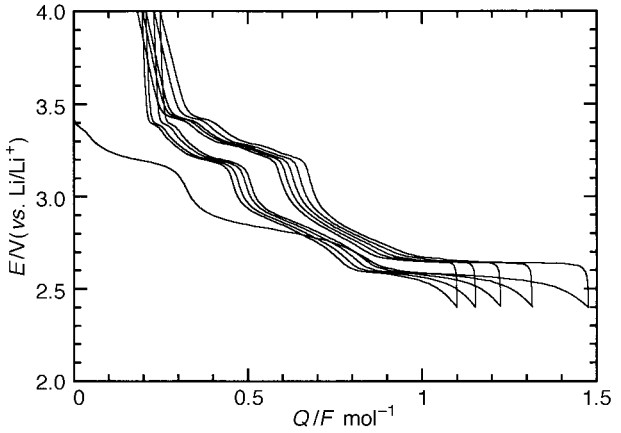

Fig. 7 Cycling galvanostatic experiments at constant current density (50 μA cm^{-2}) performed between 2.4 and 4 V on a $Ba_{0.18}V_2O_{4.95}$ electrode

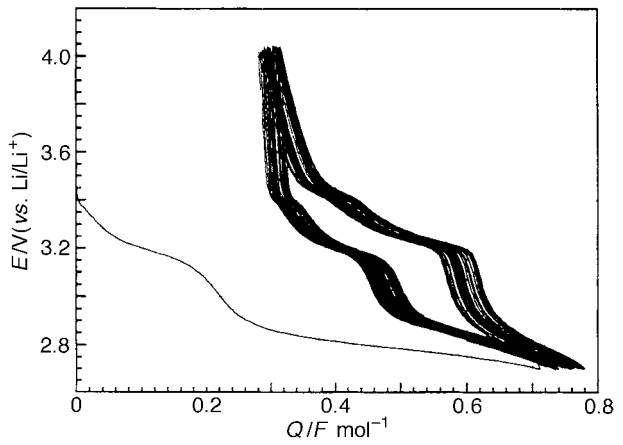

Fig. 8 Cycling galvanostatic experiments at constant current density (200 μA cm^{-2}) performed between 2.7 and 4 V on a $Ba_{0.18}V_2O_{4.95}$ electrode

Conclusion

In conclusion, two new barium-based materials belonging to the V_2O_5 group have been synthesized using the sol–gel process: an orthorhombic oxidized 'BVO' and a monoclinic reduced 'BVO', which differ both in their V^{4+} content and in their crystalline structure. This study allows, in particular, refinement of the chemical formula and the symmetry of the reduced 'BVO', which were briefly reported previously.[14]

The electrochemical investigation is in good agreement with the above data: on one hand it allows one to discriminate unambiguously the monoclinic and the orthorhombic materials, on the other hand it confirms the V^{4+} content chemically determined for the reduced 'BVO'.

Further electrochemical tests have been performed. They highlight however the poor applicability of the Ba–V oxides as rechargeable cathodic materials since they exhibit lower performances than those reported for other V_2O_5-based materials.

This result might stem from the nature (size and charge) and/or the location of the inserted barium ion, which prevent optimal filling of the lithium sites, both from a thermodynamic and a kinetic point of view. Additional structural investigations on the raw materials as well as a function of the lithium content are required to account for these observations, in particular in the case of the reduced 'BVO' for which the symmetry and the multiplicity of the lithium sites remain unknown.

References

1 J. P. Pereira-Ramos, N. Baffier and G. Pistoia in *Lithium Batteries: New Materials, Developments and Perspectives*, ed. G. Pistoia, Elsevier, Amsterdam, 1994, p. 281.
2 J. P. Pereira-Ramos, S. Bach, J. Farcy and N. Baffier, *Solid State Ionics*, 1995, **369**, 191.
3 J. P. Pereira-Ramos, *J. Power Sources*, 1995, **54**, 120.
4 S. Bach, J. P. Pereira-Ramos, N. Baffier and R. Messina, *Electrochim. Acta*, 1991, **36**, 1595.
5 P. Le Goff, N. Baffier, S. Bach and J. P. Pereira-Ramos, *J. Mater. Chem.*, 1994, **4**, 875.
6 R. Baddour, J. P. Pereira-Ramos, R. Messina and J. Périchon, *J. Electroanal. Chem.*, 1991, **314**, 81.
7 J. P. Pereira-Ramos, R. Messina, L. Znaïdi and N. Baffier, *Solid State Ionics*, 1988, **28–30**, 886.
S. Bach, J. P. Pereira-Ramos, N. Baffier and R. Messina, *J. Electrochem. Soc.*, 1990, **137**, 1042.
8 J. Livage, *Chem. Mater.*, 1991, **3**, 4; 578.
9 S. Maingot, J. P. Pereira-Ramos, N. Baffier and P. Willmann, *Solid State Ionics*, 1993, **67**, 29.
10 S. Maingot, R. Baddour, J. P. Pereira-Ramos, N. Baffier and P. Willmann, *J. Electrochem. Soc.*, 1993, **140**, L158.
11 R. Baddour, J. P. Pereira-Ramos, J. Farçy and N. Baffier, *J. Electrochem. Soc.*, 1996, **143**, 2083.
12 S. Maingot, Ph. Deniard, N. Baffier, J. P. Pereira-Ramos, A. Kahn-Harri and R. Brec, *J. Power Sources*, 1995, **54**, 342.
13 A. A. Fotiev and V. L. Volkov, *Izv. Akad. Nauk SSSR, Ser. Neorg. Mater.*, 1967, **4**, 1287.
14 A. A. Fotiev, V. V. Makarov, V. L. Volkov and L. L. Surat, *Russ. J. Inorg. Chem.*, 1969, **14** 144.
15 Y. Oka, O. Tamada, T. Yao and N. Yamamoto, *J. Solid State Chem.* 1995, **114**, 359.
16 L. Znaidi, Ph.D. Thesis, Paris VI University, 1989.
17 N. Baffier, L. Znaidi and M. Huber, *Mater. Res. Bull.*, 1990, **25**, 705.
18 N. Baffier, L. Znaidi and J. C. Badot, *J. Chem. Soc., Faraday Trans.*, 1990, **86**, 14; 2623.
19 S. Basu and W. L. Worrell, in *Fast Ion Transport in Solids*, ed. Vashita, Mundy and Shenoy, Elsevier, North Holland, 1979, p. 149.
20 J. Farcy, R. Messina and J. Perichon, *J. Electrochem. Soc.*, 1990, **137**, 1337.
21 I. D. Raistrick, *Solid State Ionics*, 1983, **9–10**, 425.
22 A. D. Wadsley, *Acta Crystallogr.*, 1955, **8**, 695.

Paper 7/07053E; *Received* 29*th September*, 1997